SLAC-PUB-3312
April 1984
(T/E)

NEW RESULTS ON RADIATIVE J/ψ DECAYS FROM MAIcK III AT SPEAR*

NORBERT WERMES
Representing the MARK III Collaboration[1]
Stanford Linear Accelerator Center
Stanford University, Stanford, California 94305

SLAC-PUB--3312
DE84 012222

Abstract

Selected topics on radiative decays of the J/ψ from MARK III at SPEAR are presented. These topics include the decay $J/\psi \to \gamma K\bar{K}$ where the final state resonances $f'(1515)$, $\theta(1700)$ and $\xi(2200)$ have been analyzed. The decay $J/\psi \to (\gamma$ vector vector) is presented in three final states, $J/\psi \to \gamma\phi\phi$, $\gamma\rho\rho$ and $\gamma\omega\omega$, providing the first measurement of the η_c spin-parity (in $\gamma\phi\phi$) and evidence for structures (in $\gamma\rho\rho$ and $\gamma\omega\omega$) near 1.7 GeV.

Invited talk presented at the XIXth Rencontre de Moriond:
New Particle Production, La Plagne, France, March 4-10, 1984

*Work supported in part by the Department of Energy, contract DE-AC03-76SF00515, and by the Alexander von Humboldt Foundation, Germany.

1. Introduction

QCD inspired models predict gluon bound states (glueballs) in the energy region between 0.5 and 3 GeV.[2] Radiative decays of the J/ψ have always been argued to be an ideal place to search for such glueballs.[3] This is because the reaction $J/\psi \to \gamma + X$ proceeds as depicted in fig. 1 where the decay to the hadronic final state X is mediated by two gluons. Such states are expected to be produced with a branching fraction of order α/α_s,[4]

$$\frac{\Gamma(J/\psi \to \gamma gg)}{\Gamma(J/\psi \to ggg)} = \frac{16\alpha}{5\alpha_s}\left[1 + O\left(\frac{\alpha_s}{\pi}\right)\right] \approx (6-10)\% \quad . \tag{1}$$

The MARK III detector at SPEAR has collected and analyzed $2.7 \times 10^6 J/\psi$ decays. The analysis effort has concentrated mainly on radiative decays. New results on the decay $J/\psi \to \gamma K\bar{K}$, with evidence for a new narrow state around 2.2 GeV, have been presented recently.[5] This report will present further analysis of this decay mode.

The radiative decay of the J/ψ into two vector particles has so far only been analyzed by MARK II[6] in the reaction $J/\psi \to \gamma\rho^0\rho^0$. Here analyses on $J/\psi \to \gamma\phi\phi$, $\gamma\rho\rho$ and $\gamma\omega\omega$ will be presented which provide the first determination of the η_c spin-parity (in $\gamma\phi\phi$) and the observation of structures around 1.7 GeV (in $\gamma\rho\rho$, $\gamma\omega\omega$).

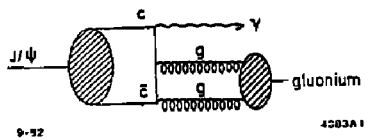

Fig. 1. Diagrammatic representation of the radiative J/ψ decay to gluonium in lowest order QCD.

2. The Detector

The MARK III detector is a 4π-magnetic detector dedicated for J/ψ and charm physics at the e^+e^- storage ring SPEAR. The detector is described in detail elsewhere.[7] The most important features, necessary for reconstruction and analysis of exclusive final states, are listed below:

i. charged particle acceptance over 84% of 4π,

ii. acceptance for photons over 94% of 4π,

iii. good momentum resolution for charged particles $\sigma_p/p = 1.5\% \cdot \sqrt{1+p^2}$, p in GeV/c,

iv. good spatial resolution and sufficient energy resolution for photons ($\sigma_\phi = 7$ mr, $\sigma_\theta = 10$ mr, $\sigma_E/E = 17\%/\sqrt{E}$, E in GeV),

v. very good low energy photon efficiency ($\sim 100\%$ for $E_\gamma > 100$ MeV),

vi. good particle identification by TOF ($\sigma_{TOF} = 189$ *ps* over 81% of 4π) and dE/dx.

The momentum and energy resolutions are improved substantially by kinematic fitting. This technique is used for all the topics presented in this report and has been successfully applied to final states with up to five photons and four charged tracks.

3. $J/\psi \to \gamma K\bar{K}$

The decay $J/\psi \to \gamma K\bar{K}$ has been analyzed by requiring good 4-C fits and TOF identification of the kaons. The K^+K^- mass distribution in shown in fig. 2(a). Three prominent peaks due to the $f'(1515)$, the $\theta(1709)$ and the $\xi(2200)$ are evident. The f' and θ appear well separated in this analysis and one finds

$$\begin{aligned} m_{f'} &= (1525 \pm 10)\,\text{MeV}, \qquad \Gamma_{f'} = (85 \pm 25)\,\text{MeV}, \\ m_\theta &= (1720 \pm 10)\,\text{MeV}, \qquad \Gamma_\theta = (130 \pm 25)\,\text{MeV}, \end{aligned} \tag{2}$$

when fitting with two incoherent Breit-Wigner curves. The branching fractions were determined to be

$$\begin{aligned} B(J/\psi \to \gamma f')\, B(f' \to K^+K^-) &= (3.0 \pm 0.7 \pm 0.8) \times 10^{-4}, \\ B(J/\psi \to \gamma \theta)\, B(\theta \to K^+K^-) &= (4.5 \pm 0.6 \pm 0.9) \times 10^{-4}. \end{aligned} \tag{3}$$

Figure 2(b) shows the KK mass plot for selected $J/\psi \to \gamma K^0_s K^0_s$ events. The number of observed events agrees with the expectation from γK^+K^-. Although the statistics in this decay mode is very marginal, fig. 2(b) supports the observation of the peaks in fig. 2(a).

The Dalitz plot for $J/\psi \to \gamma K^+K^-$ is shown in fig. 3. Apart from the three diagonal bands due to f', θ, and ξ, there are also visible background bands from the direct decay $J/\psi \to K^*K$.

A spin-parity analysis has been performed for the f' using a maximum likelihood method. The quantum numbers of the K^+K^- system are restricted to the sequence 0^{++}, 2^{++}, ... because production in radiative J/ψ decays implies $C = +1$, and for two spinless bosons $C = P = (-1)^L$. For the f', which has a fairly low mass, only the 0^{++} and 2^{++} hypotheses were allowed in the fit. The spin 2 angular distribution is parametrized by allowing the helicity amplitude ratios, $x = A_1/A_0$ and $y = A_2/A_0$, to be complex as has been suggested by Körner.[3]

We find that spin 2^{++} is preferred over 0^{++} with significance $> 10^3$. The phases of x and y are found to be consistent with zero and x, y are measured to be $x = 0.7 \pm 0.1$,

$y = 0.02 \pm 0.2$ in quite remarkable agreement with the values obtained[8] for the $f(1270)$ ($x = 0.77 \pm 0.05$, $y = 0.01 \pm 0.06$). The fit finds a second minimum around $x \sim -0.7$, $y \sim 0$ reflecting a sign ambiguity in x.

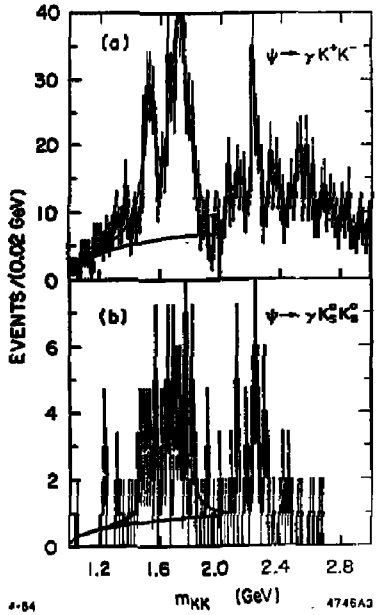

Fig. 2. $\text{Mass}_{(KK)}$ (GeV) distribution for (a) $J/\psi \to \gamma K^+K^-$, and for (b) $J/\psi \to \gamma K^0_S K^0_S$. The curves represent fits to two incoherent Breit-Wigner curves plus a quadratic background.

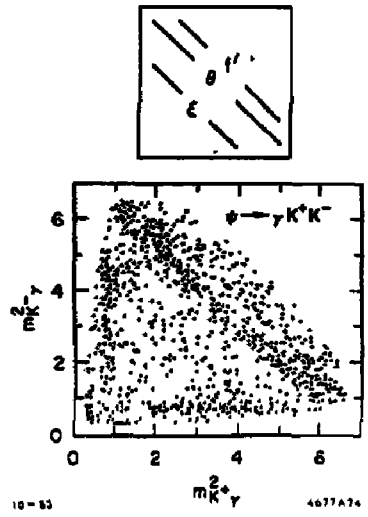

Fig. 3. Dalitz plot of $\text{mass}^2_{(K^+\gamma)}$ (GeV^2) versus $\text{mass}^2_{(K^-\gamma)}$ (GeV^2) from $J/\psi \to \gamma K^+K^-$. The schematic drawing displays the bands of the $f'(1515)$, θ and ξ decays.

This result is interesting in two respects:

1. The assumption in previous J^P determinations of f, f', that x and y are real, seems to be justified.
2. The measurement of x, y for $f(1270)$ and $f'(1515)$ can be compared to a conjecture made by F. Close[9] predicting that 2^{++} $q\bar{q}$ states should have $x \sim \sqrt{3}/2$, $y \sim 0$. This is in remarkable agreement with the data. A detailed calculation by Koerner et al.[10] predicts that for the $f'(1515)$: $\phi_x = 1.3°$, $\phi_y = 2.4°$, $x = 0.9$, $y = 0.72$.

For the $\theta(1700)$ the spin-parity analysis is still in progress because the distinction between the 0^{++} and 2^{++} hypotheses is more ambiguous than for the f'.

Figure 4 shows the evidence for the new state ξ around 2.2 GeV in the K^+K^- mass distribution. We observe 29 events above a background of approximately 23 events in the

total data sample of 2.7×10^6 ψ decays. A fit to the [2.0 – 2.5 GeV] mass region with a polynomial background assuming no signal yields a significance of 4.6σ for this resonance.

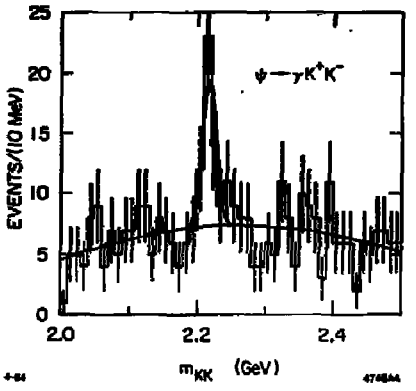

Fig. 4. Mass$_{(K^+K^-)}$ (GeV) distribution from $J/\psi \to \gamma K^+K^-$ above 2 GeV. The curve represents a fit to a Breit-Wigner convoluted with a Gaussian plus a quadratic background.

Because the measured width is consistent with the experimental mass resolution, a Breit-Wigner curve folded with a Gaussian has been fitted to the signal yielding

$$m_\xi = (2218 \pm 3 \pm 10)\ \text{MeV}\ ,$$
$$\Gamma_\xi < 40\ \text{MeV}\ \ (95\%\ \text{C.L.})\ . \qquad (4)$$

The branching ratio has been determined using $J = 2$, $x = 1$, $y = 1$ to be

$$B(J/\psi \to \gamma\xi)\, B(\xi \to K^+K^-) = (5.8 \pm 1.8_{stat} \pm 1.5_{sys}) \times 10^{-5}\ . \qquad (5)$$

The systematic error includes the change in the efficiency when using different assumptions for J, x and y.

One difficulty we have had in this analysis is that the number of observed events recorded in the 1982 running period is somewhat less than the expected number based on the data sample recorded later.

The total sample of 2.7×10^6 ψ decays was collected in about six weeks of running in 1982 ($\sim 0.9 \times 10^6$ ψ decays) and about five weeks of running in 1983 ($\sim 1.8 \times 10^6$ ψ decays). The two different sets of data are shown individually in figs. 5(a),(b) with the relative proportions

of 0.8 : 1.8 . The overplotted curve in fig. 5(a) is the expectation from the 1983 data (fig. 5(b)) scaled to the 1982 data.

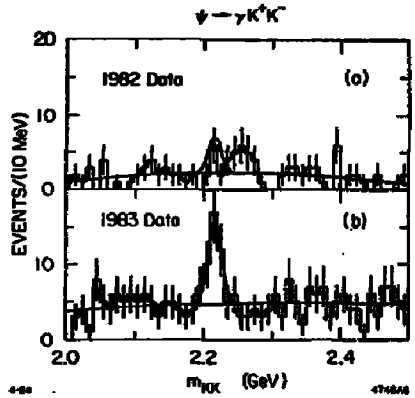

Fig. 5. $\text{Mass}_{(K^+K^-)}$ (GeV) distributions for the two data samples taken (a) in 1982 ($\sim 0.9 \times 10^6$ ψ decays) and (b) in 1983 ($\sim 1.8 \times 10^6$ ψ decays). The curve in (a) is what one would expect scaling the signal from the 1983 data as fitted in (b) to the 1982 data.

We believe that we can rule out any systematic difference between the two sets of data. On a statistical basis we expect, assuming a mass and width as determined from the 1983 sample, eleven events in the 1982 data and we observe four. This corresponds to about 2.2 standard deviations in the difference. The statistical significance of the 1983 data alone is 5σ.

In the $K_s^oK_s^o$ decay mode (fig. 2(b)) 6 events are observed above a background of 4 events. This supports the finding in the K^+K^- mode although with very poor statistics. The branching ratio in the $K_s^oK_s^o$ mode agrees with eq. (5).

The observation of a narrow resonance above 2 GeV has given rise to many theoretical speculations about its origin.[11,12] Apart from the measurement of the width, eq. (4), the spin determination is very important to supply more information about this object.

The $\gamma K\bar{K}$ final state is completely described by the particle momenta and three angles, $\cos\theta_\gamma$ of the γ in the lab frame and $\cos\theta_K^*$ and φ_K^* of the kaons in the $K\bar{K}$ center of mass frame. θ_γ and φ_K^* are affected by large acceptance corrections, whereas θ_K^* is not because it is the only true center of mass angle for this decay. The $\cos\theta_K^*$ distribution is shown in fig. 6(a). The distribution is essentially flat with some population of events at the ends. This would offer hope for a spin determination.

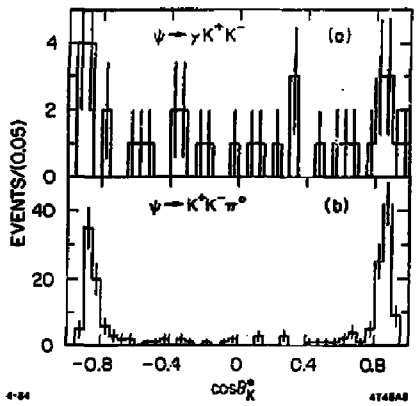

Fig. 6. Distributions of $\cos\theta^*_K$ for (a) $J/\psi \to \gamma K^+K^-$ events at the mass of the $\xi(2200)$ and (b) for background events from $J/\psi \to K^*K \to K^+K^-\pi^0$.

However, as can be seen from fig. 3, the $J/\psi \to K^*K$ background events populate the boundary of the Dalitz plot and hence correspond to $|\cos\theta^*_k| \sim 0.8$–$1.0$. This is demonstrated in fig. 6(b) where the same angle is plotted for selected $K^+K^-\pi^0$ events.

Therefore we must conclude that with present statistics the spins $J^P = 0^{++}, 2^{++}, 4^{++}$ are indistinguishable at the 2σ level due to a) a small signal, b) a poor signal-to-noise ratio, and c) the presence of the K^*K background.

Among the many theoretical speculations about the ξ, a Higgs particle assignment[11] seems to be the most exciting. To examine this question we have searched for the ξ in the decay $J/\psi \to \gamma\mu\mu$, and also in $J/\psi \to \gamma\pi^+\pi^-$, $J/\psi \to \gamma K^*K$, $J/\psi \to \gamma K^*K^*$, $J/\psi \to \gamma\eta\eta$, and $J/\psi \to \gamma p\bar{p}$, which may be relevant to other models, too. We find no evidence for structure around 2.2 GeV and place the following upper limits:

$$\left.\begin{aligned}
B(J/\psi \to \gamma\xi(2.2)) \cdot B(\xi(2.2) \to \mu^+\mu^-) &< 7.3 \times 10^{-6} \\
B(J/\psi \to \gamma\xi(2.2)) \cdot B(\xi(2.2) \to \pi^+\pi^-) &< 3 \times 10^{-5} \\
B(J/\psi \to \gamma\xi(2.2)) \cdot B(\xi(2.2) \to K^*K) &< 2.5 \times 10^{-4} \\
B(J/\psi \to \gamma\xi(2.2)) \cdot B(\xi(2.2) \to K^*\bar{K}^*) &< 3 \times 10^{-4} \\
B(J/\psi \to \gamma\xi(2.2)) \cdot B(\xi(2.2) \to \eta\eta) &< 7 \times 10^{-5} \\
B(J/\psi \to \gamma\xi(2.2)) \cdot B(\xi(2.2) \to p\bar{p}) &< 6 \times 10^{-5}
\end{aligned}\right\} \quad 90\%\ C.L.$$

On the basis of our data a standard Higgs assignment seems to be rather unlikely because (a)

the mass is much lower than the Linde-Weinberg bound[13], which demands $m_H > 7$ GeV in order that the Standard Model is stable against radiative corrections, (b) the measured rate to $K\bar{K}$ $((11.6 \pm 3.6 \pm 3.0) \times 10^{-5})$ for the product branching ratio is larger than expected for $J/\psi \to \gamma H^0$ using the Wilczek mechanism[14]

$$B(\psi \to \gamma H^0) = \frac{G_f m_\psi^2}{4\sqrt{2}\pi\alpha}\left(1 - \frac{m_H^2}{m_\psi^2}\right) \cdot B(\psi \to \mu^+\mu^-)$$

$$\approx 3 \times 10^{-6} \ ,$$

and (c) the relative rate for $B(H^0 \to \mu\mu)/B(H^0 \to s\bar{s})$ expected to be 4–16 %,[12] depending on the assumed s-quark mass, is measured to be

$$\frac{B(\xi \to \mu\mu)}{B(\xi \to s\bar{s})} < 6\% \cdot \frac{B(\xi \to K\bar{K})}{B(\xi \to s\bar{s})} .$$

A more extensive discussion on whether the ξ(2200) could be a Higgs boson including models with more than one Higgs doublet is presented in ref. 15.

4. $J/\psi \to \gamma$ Vector Vector

4.1 $J/\psi \to \gamma\eta_c$, $\eta_c \to \phi\phi$ [16]

In the decay $J/\psi \to \gamma K^+K^-K^+K^-$ clear evidence for $\phi\phi$-production is observed (fig. 7). The $\phi\phi$ mass is plotted in fig. 8 showing 18 η_c events above a background of 1–2 events. The mass is 2976±8 MeV and the observed width is consistent with the mass resolution of 20 MeV.

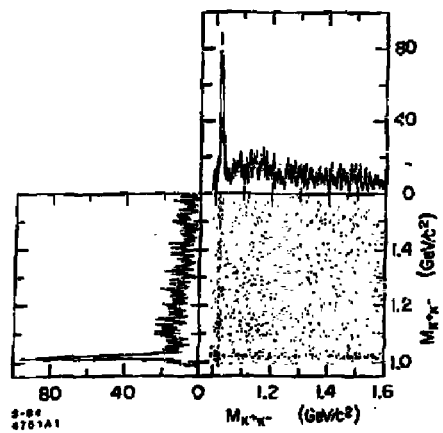

Fig. 7. Scatterplot of $m_{(K^+K^-)}(1)$ (GeV) versus $m_{(K^+K^-)}(2)$ (GeV) providing evidence for $\phi\phi$ production in $J/\psi \to \gamma 4K$.

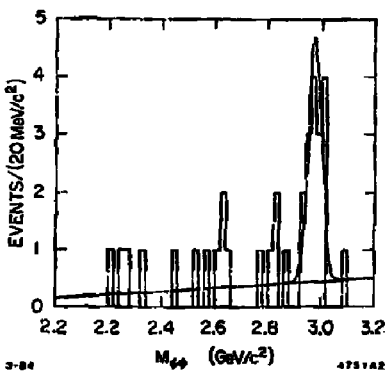

Fig. 8. Mass$_{\phi\phi}$ (GeV) distribution from $J/\psi \to \gamma\phi\phi$. The detection efficiency decreases from ~ 6% at 3 GeV to zero at 2 GeV.

The branching ratio is

$$B(\eta_c \to \phi\phi) = (8.0 \pm 2.0 \pm 2.5) \times 10^{-3} \quad , \tag{6}$$

using $B(\psi \to \gamma\eta_c) = (1.27 \pm 0.36) \times 10^{-2}$ as measured by Crystal Ball.[17]

It has been pointed out by Chang and Nelson[18] and Trueman[19] that the $\phi\phi$ decay of the η_c provides a maximal parity signature for the η_c exploiting the information buried in the orientation of the two ϕ decay planes. This is analogous to Yang's parity test[20] for the π^0. That is, the ϕ decay planes are preferentially orthogonal for odd parity and parallel for even parity. The distribution of the angle between these planes (χ) takes the form[18]

$$\frac{d\sigma}{d\chi} = 1 + \beta \cos(2\chi) \quad , \tag{7}$$

where β is a constant which depends only on spin and parity and is independent of the polarization of the $\phi\phi$ system.

Figure 9 shows the χ distribution for the η_c events. The expectations for several spin-parity assignments are overplotted. Quantitatively we show in Table I that 0^- is the preferred assignment for the η_c spin-parity.

Table I

Likelihood ratios of 0^- with respect to J^P for the η_c. The fits exploit the χ angle information only. The numbers in parentheses are based on fits to χ, $\cos\theta_{K_1}$ and $\cos\theta_{K_2}$ distributions.

J^P	$L_{\phi\phi}$	$S_{\phi\phi}$	β_{theory}	Likelihood Ratio
0^-	1	1	−1.	1
0^+	0	0	+.667	1.8×10^8
0^+	2	2	+.333	1.8×10^5
1^-	1	1	0.	2200
1^+	2	2	0.	2200
2^-	1	1	−.4	55 (4400)
2^-	3	1	−.6	12 (120)
2^+	0	2	+.07	5100

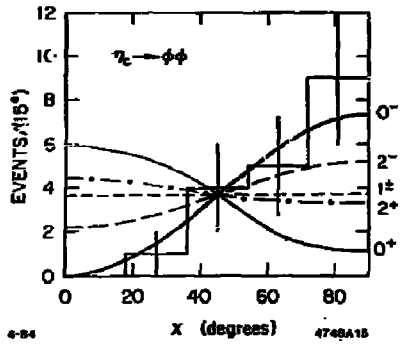

Fig. 9. Distribution of χ, the angle between the ϕ decay planes from $\eta_c \to \phi\phi$ events. The curves represent the expectations from 0^- (thick solid), 0^+ (solid), 1^* (short dashed), 2^+ (dashed dotted) and 2^- (long dashed).

4.2 $J/\psi \to \gamma\rho\rho$

The Mark II[6] has measured the decay $J/\psi \to \gamma\pi^+\pi^-\pi^+\pi^-$. They observe resonance structure around 1.65 GeV with a large $\rho^0\rho^0$ component ($B(\psi \to \gamma\rho^0\rho^0) = (1.25 \pm 0.35 \pm 0.40) \times 10^{-3}$ for $m_{4\pi} < 2$ GeV). If this was mainly due to the decay $\theta \to \rho^0\rho^0$ then the total branching fraction for $J/\psi \to \gamma\theta$ would be very big and a glueball assignment for the θ would be very tempting.

In $\gamma\gamma$ reactions a large cross section has been measured[21],[22] between 1.4 and 1.8 GeV in $\gamma\gamma \to \rho^0\rho^0$. The cross section in $\gamma\gamma \to \rho^+\rho^-$ is much smaller,[23] by at least a factor five, in this mass range. An angular correlation analysis in $\gamma\gamma \to \rho^0\rho^0$ rules out large contributions from a 0^- or 2^- spin-parity assignment. Instead the data are consistent with sizeable contributions from 0^+ for $m_{4\pi} < 1.7$ GeV and 2^+ for $m_{4\pi} > 1.7$ GeV, but they are also consistent with isotropic production and decay of the ρ's.

In this context the MARK III has analyzed $J/\psi \to \gamma 4\pi$ in the two modes $J/\psi \to \gamma\pi^+\pi^-\pi^+\pi^-$ and $J/\psi \to \gamma\pi^+\pi^-\pi^0\pi^0$. The analysis is still preliminary. Events have been selected requiring four charged tracks and one photon, and two charged tracks and five photons, respectively. They have then been kinematically fitted to the corresponding $J/\psi \to \gamma 4\pi$ hypothesis.

Figures 10(a),(b) show the 4π mass distributions for both decay modes. In both cases structure is observed, above a large background from $J/\psi \to 5\pi$ events, between 1.5 and

1.9 GeV. Cuts on the χ^2 of the kinematic fits, on the number of good photons, and on

$$p_{T\gamma}^2 = 4 \cdot |\vec{p}_{4\pi}|^2 \cdot \sin^2 \theta/2 \quad ,$$

where θ is the angle between the radiative photon and the measured momentum vector of the four pion system, reduce this background to below 10% for the $J/\psi \to \gamma\pi^+\pi^-\pi^+\pi^-$ final state.

In fig. 11(a) the scatterplot of the two oppositely charged $\pi\pi$ mass combinations is shown with two entries per event. Figure 11(b) shows the corresponding correlation for equally charged $\pi\pi$ pairs. A sizeable $\rho\rho$ component is evident from these plots. The black dot in the lower left corner of fig. 11(a) corresponds to $K_S^0K_S^0$ events which were removed from the sample afterwards.

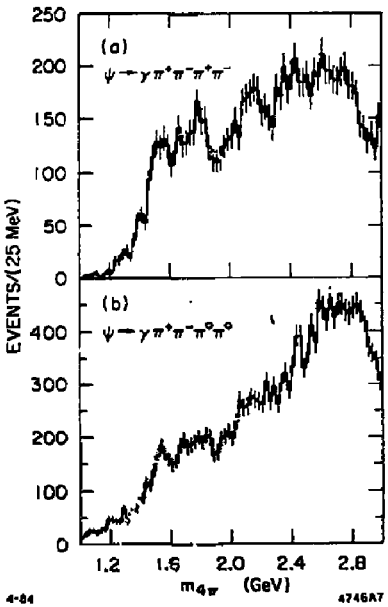

Fig. 10. Mass(4π) (GeV) distributions from (a) $J/\psi \to \gamma\pi^+\pi^-\pi^+\pi^-$ and (b) $J/\psi \to \gamma\pi^+\pi^-\pi^0\pi^0$. Kinematical cuts to suppress background have not yet been applied.

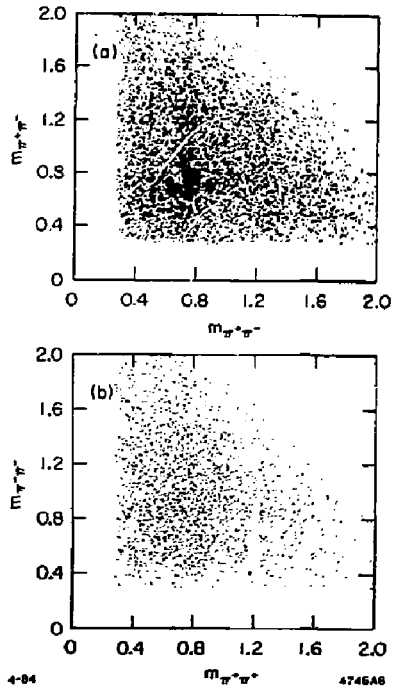

Fig. 11. Scatterplot of (a) $m_{(\pi^+\pi^-)}(1)$ (GeV) versus $m_{(\pi^+\pi^-)}(2)$ (GeV) with two entries per event and (b) $m_{(\pi^+\pi^+)}$ (GeV) versus $m_{(\pi^-\pi^-)}$ (GeV) providing evidence for $\rho^0\rho^0$ production in $J/\psi \to \gamma\pi^+\pi^-\pi^+\pi^-$.

In order to separate the contributions from $\rho\rho$, $\rho\pi\pi$ and 4π, maximum likelihood fits have been applied that include possible resonance production in $\rho\rho$ with several spin-parity assignments.

The four pion final state is defined by seven angles and two masses: the angle θ_γ of the photon in the lab frame, the ρ production angles θ_ρ, φ_ρ defined in the X helicity frame, the angles of the ρ decays θ_{π_1}, φ_{π_1}, θ_{π_2}, φ_{π_2} in the ρ helicity frames, and the two $\pi\pi$ masses. For the radiative decay $J/\psi \to \gamma X$ the matrix element $T_{m\lambda}$, where m is the J/ψ polarization and λ the helicity of the radiative photon, is given by

$$T_{m\lambda} = A_0 \frac{m+\lambda\cos\theta_\gamma}{2} F_0 - A_1 \frac{\sin\theta_\gamma}{\sqrt{2}} F_\lambda + A_2 \frac{m-\lambda\cos\theta_\gamma}{2} F_{2\lambda} \quad . \tag{8}$$

$A_{0,1,2}$ are the production and F_λ the decay amplitudes for the process. For X decaying into two ρ's which in turn decay into 4 pions, the decay amplitudes include the ρ Breit-Wigner amplitudes as

$$F_\lambda = \frac{1}{\sqrt{2}} \sum_{k=1}^{2} BW(k) \cdot G_\lambda(k) \quad , \tag{9}$$

where $BW(k)$ stands for the product of the two ρ Breit-Wigner amplitudes of $\pi\pi$ combination k. $G_\lambda(k)$ is given by

$$G_\lambda(k) = \sum_{i,j=-1}^{1} B_{ij}\, D^1_{j0}\left(\Omega^k_{\pi_1}\right) \cdot D^1_{j0}\left(\Omega^k_{\pi_2}\right) \cdot D^{J_X}_{\lambda,i-j}\left(\Omega^k_\rho\right) \quad , \tag{10}$$

with $\Omega = (\theta, \varphi)$. B_{ij} are the relative helicity amplitudes for the decay which can be calculated for a given J^P. The D's represent the standard rotation matrices.

Using this formalism the data have been fitted by considering 10 different channels: isotropic $\rho\rho$, $\rho\pi\pi$, 4π; $\rho\rho$ with $J^P = 0^+, 0^-, 1^+, 1^-, 2^+, 2^-$, and a background channel due to $A_1\pi$ production. The following assumptions have been made when performing the fit:

1. The production amplitudes A_i had to be relatively real, i.e. x,y had to be real.
2. Only the lowest possible angular momentum was considered for a given J^P.
3. No interference was allowed between the amplitudes of different channels.

For the 4π mass range from 1.5 to 1.9 GeV, fig. 12(a) shows the distribution of χ, the angle between the ρ decay planes, defined in exactly the same way as for $\eta_c \to \phi\phi$ but now with two entries per event. The shape of this distribution is not flat and very much reminiscent of that in fig. 9, indicating a large contribution from even spin and odd parity. Figure 12(b) shows a flat distribution of the same angle for $2.8 \leq m_{4\pi} \leq 2.95$ GeV.

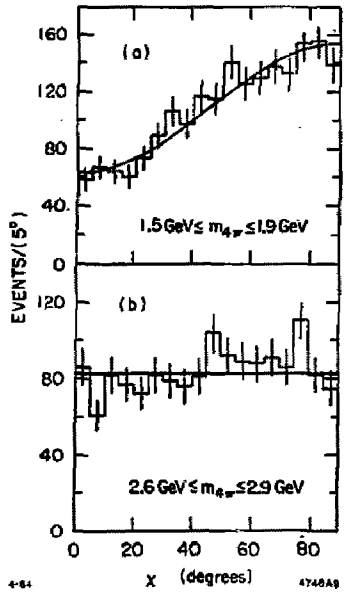

Fig. 12. The χ–angle distribution from $J/\psi \to \gamma\pi^+\pi^-\pi^+\pi^-$ for (a) 1.5 GeV$\leq m_{4\pi} \leq$ 1.9 GeV and (b) 2.6 $\leq m_{4\pi} \leq$ 2.9 GeV. A fit to (a) with $a + b\sin^2\chi$ yields $a = 62.7 \pm 3.5$, $b = 90.2 \pm 6$ and $\chi^2 = 13.7$ with 16 d.o.f. .

The results of the 10-channel fit confirm this observation as demonstrated in figs. 13(a)-(j). The fitted contributions of each channel are plotted as a function of $m_{4\pi}$. Apart from a large non-resonant 4π contribution, the shape of which agrees with $\gamma 4\pi$ and 5π phase space expectations, we find also a large 0^- contribution which amounts to about 50% of the data between 1.5 and 1.9 GeV. This observation is insensitive to the number of channels allowed in the fit. We also find that the contribution from 2^+ is less than about 20% in the θ mass region and not significant in the mass region between 2 and 2.4 GeV. Thus, there is no evidence here for the three 2^{++} states found by the BNL/CCNY collaboration in the process $\pi^- p \to \phi\phi n$[24].

The 0^- projection (fig. 13 (e)) of the fit results is again shown in fig. 14(a) with a different binning. Figure 14(b) shows the same distribution for the corresponding analysis in the decay $J/\psi \to \gamma\rho^+\rho^-$.

The following preliminary branching ratios are obtained

$$B(\psi \to \gamma\pi^+\pi^-\pi^+\pi^-) = (6 \pm 2) \times 10^{-3} \text{ for } 1GeV < m_{4\pi} < 3GeV,$$
$$B(\psi \to \gamma X(1.5-1.9, 0^-)) \cdot B(X \to \rho^0\rho^0) = (7.7 \pm 3.0) \times 10^{-4}. \quad (11)$$

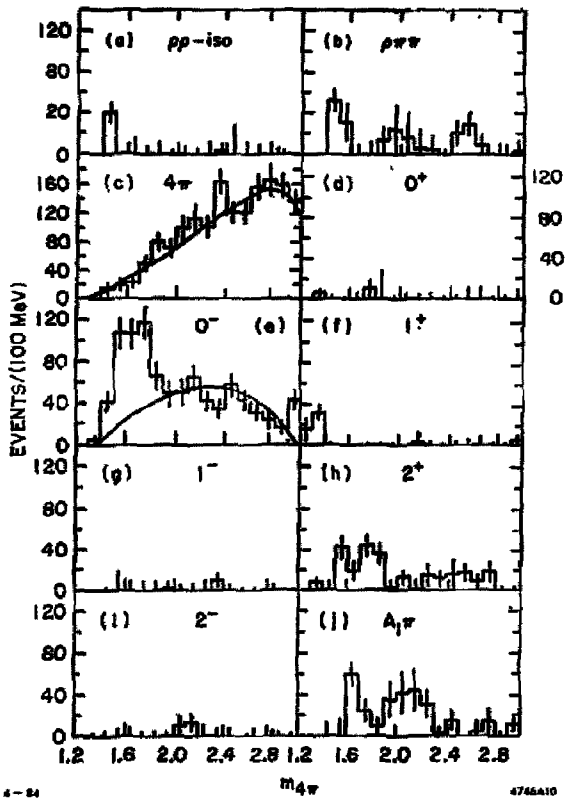

Fig. 13. Preliminary results of a 10-channel spin-parity analysis on $J/\psi \to \gamma\pi^+\pi^-\pi^+\pi^-$ events. Plotted is mass$_{(4\pi)}$ (GeV) weighted with the fraction of the corresponding channel as determined by the fit. The curves drawn in (c) and (e) represent phase space for (c) $J/\psi \to \gamma 4\pi$, and (e) $J/\psi \to \gamma\rho\rho$, respectively.

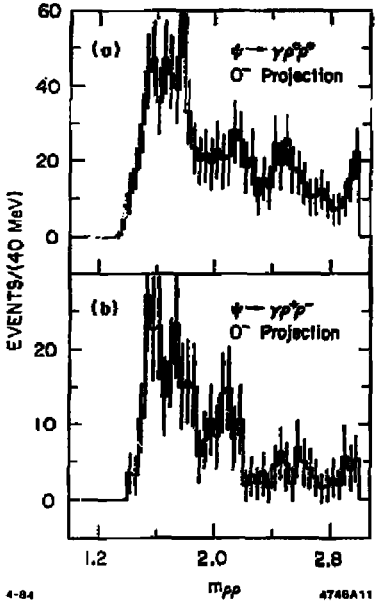

Fig. 14. Mass$_{\rho\rho}$ (GeV) distribution weighted with 0^- channel weight. ($\rho\rho - 0^-$ projection) for (a) $J/\psi \to \gamma\rho^0\rho^0$ and (b) $J/\psi \to \gamma\rho^+\rho^-$ (preliminary).

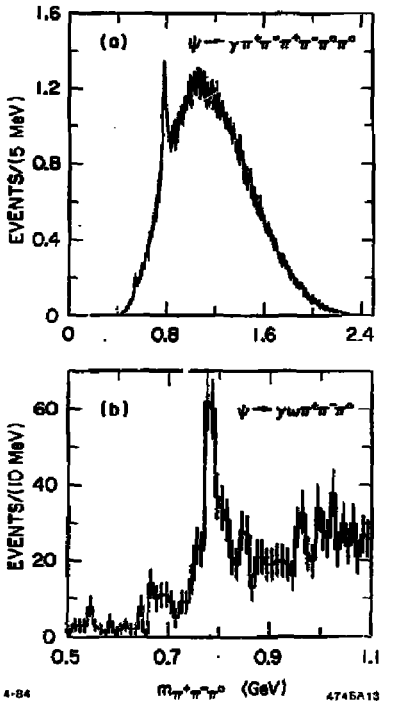

Fig. 15. Mass$_{\pi^+\pi^-\pi^0}$ (GeV) distribution (a) for eight combinations per event from $J/\psi \to \gamma\pi^+\pi^-\pi^+\pi^-\pi^0\pi^0$ and (b) for the recoiling $\pi^+\pi^-\pi^0$ combination after requiring 0.753 GeV $\leq m_{(\pi^+\pi^-\pi^0)} \leq$ 0.813 GeV for one combination in (a).

4.3 $J/\psi \to \gamma\omega\omega$

The decay $J/\psi \to \pi^+\pi^-\pi^+\pi^-\pi^0\pi^0$ has been analyzed applying 4C and 6C fits, exploiting the two π^0 mass constraints, to events with four charged tracks and 5 photons. Figure 15(a) shows the invariant $\pi^+\pi^-\pi^0$ mass distributions. Clear ω and η signals are evident mainly coming from $J/\psi \to \omega\pi^+\pi^-\pi^0\pi^0$ and $J/\psi \to \omega\eta$. After requiring 0.753 GeV $\leq m_{\pi^+\pi^-\pi^0} \leq$ 0.813 GeV for one $\pi^+\pi^-\pi^0$ combination the mass of the recoiling 3 pion system is plotted in fig. 15(b). Clear evidence for $\omega\omega$ production is presented in figs. 16(a),(b), where four of the $\pi^+\pi^-\pi^0$ mass combinations are histogrammed against the four recoiling combinations (4 entries per event). Figure 16 (a) includes the full 6π mass range, whereas the events in fig. 16 (b) are restricted to 1.6 GeV$\leq m_{6\pi} \leq$ 1.9 GeV. Because the processes $J/\psi \to \omega\omega$ and $J/\psi \to \pi^0\omega\omega$ are forbidden by C–invariance, the presence of the two ω's in the event is direct evidence for the radiative decay $J/\psi \to \gamma\omega\omega$.

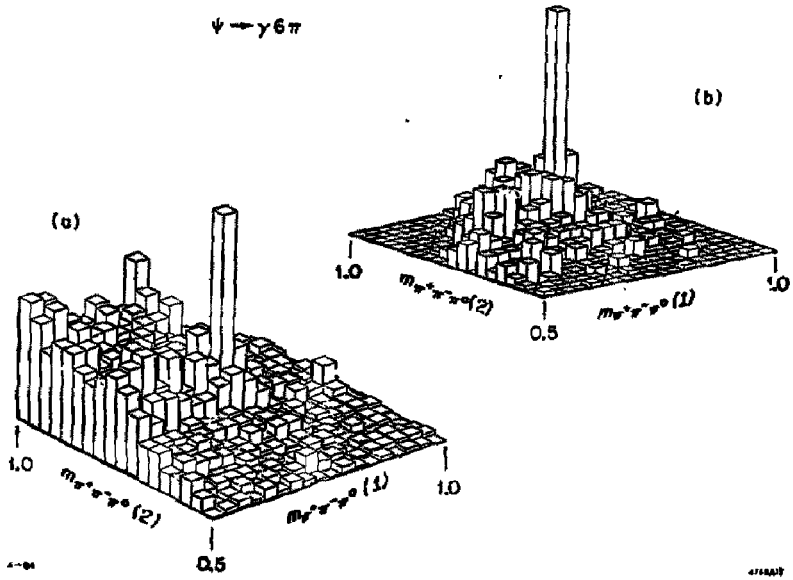

Fig. 16. Three dimensional histogram of $m_{\pi^+\pi^-\pi^0}(1)$ versus $m_{\pi^+\pi^-\pi^0}(2)$ in (GeV) from $J/\psi \to \gamma\pi^+\pi^-\pi^0\pi^+\pi^-\pi^0$ (four entries per event) for (a) all 6π-masses and (b) 1.8 GeV$\leq m_{6\pi} \leq$ 1.9 GeV.

After selecting two ω's (0.753 GeV$\leq m_{\pi^+\pi^-\pi^0} \leq$ 0.813 GeV), $m_{\omega\omega}$ is plotted in fig. 17 before (a) and after (b) background subtraction. The amount of background (shaded area) has been determined from the ω-sidebands. The shape of the $m_{\omega\omega}$ mass distribution is similar to the 0^{-+}-projection for $J/\psi \to \gamma\rho\rho$ (fig. 14). It is different, however, from $J/\psi \to \gamma\omega\omega$ phase space (dashed line). Structure is again observed between 1.8 and 1.9 GeV cutting off sharply at the $\omega\omega$ threshold.

Here again the χ angle is a useful tool to obtain spin-parity information. The χ angle can be calculated similarly to $J/\psi \to \gamma\rho\rho$ and $J/\psi \to \gamma\phi\phi$ but using the normal to the $\pi^+\pi^-\pi^0$ plane in the respective ω rest frames. In fig. 18 the χ angle is plotted for (a) $J/\psi \to \gamma\omega\omega$ with $1.6 \leq m_{\omega\omega} \leq 1.9$ GeV with the background subtracted, for (b) the ω sidebands, and for (c) $2.4 \leq m_{\omega\omega} \leq 2.8$ GeV. The shape of fig. 18(a) is inconsistent with odd spin or even parity, but consistent with 0^{-+} or 2^{-+}. This suggests that the structures observed in $J/\psi \to \gamma\rho\rho$ and $J/\psi \to \gamma\omega\omega$ have the same origin. A fit with $a + b\sin^2\chi$ yields $a = 4.7 \pm 0.3, b = 13.6 \pm 0.5$ (*i.e.*, 58% $\sin^2\chi$) with $\chi^2 = 2.1$, 4 d.o.f.; a fit with a constant yields $\chi^2 = 10.3$ with 5 d.o.f. We obtain the following preliminary branching fractions:

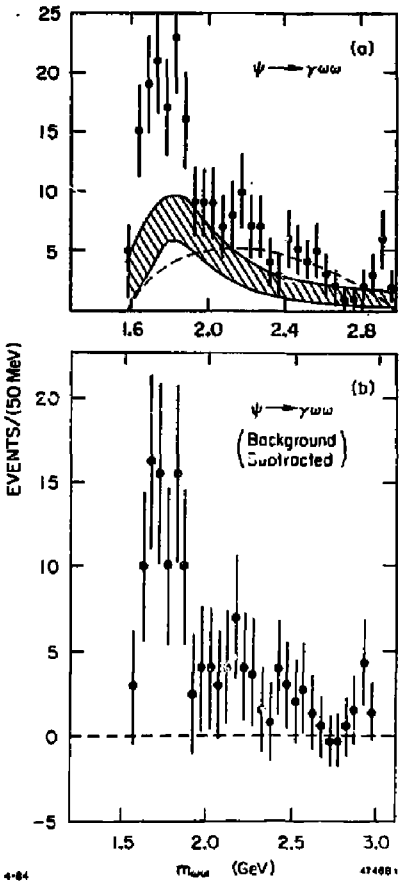

Fig. 17. Mass$_{(\omega\omega)}$ (GeV) distributions from $J/\psi \to \gamma\omega\omega$ (a) before and (b) after background subtraction as determined from the ω sidebands. The dashed line represents a $J/\psi \to \gamma\omega\omega$ phase space calculation.

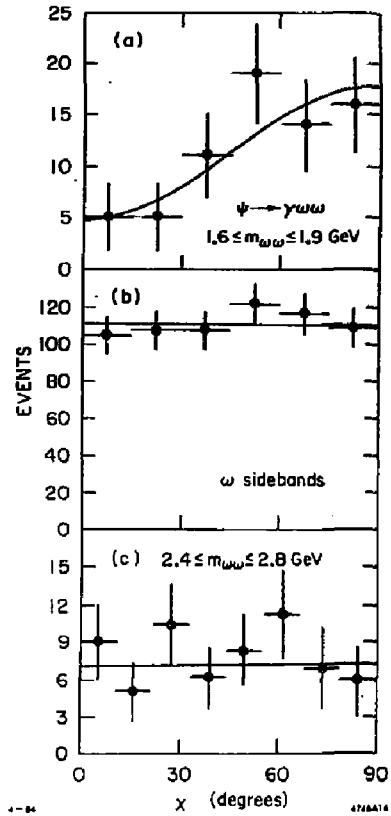

Fig. 18. The χ–angle distribution from $J/\psi \to \gamma\omega\omega$ (a) for 1.6 GeV $\leq m_{\omega\omega} \leq$ 1.9 GeV, background subtracted, (b) for events from the ω sidebands, and (c) for 2.4 GeV$\leq m_{\omega\omega} \leq$ 2.8 GeV. The curves represent fits with (a) $a + b\sin^2\chi$, $a = 4.7 \pm 0.3$, $b = 13.0 \pm 0.5$, $\chi^2 = 2.1$, 4 d.o.f. and (b), (c) constants. (preliminary)

$$B(\psi \to \gamma\omega\omega) = (8.8 \pm 1.8 \pm 2.4) \times 10^{-4} \quad \text{for} \quad 1\ \text{GeV} \leq m_{\omega\omega} \leq 3\ \text{GeV}$$

$$B(\psi \to \gamma\omega\omega) = (7.5 \pm 5.0 \pm 2.0) \times 10^{-5} \quad \text{for} \quad 2.0\ \text{GeV} \leq m_{\omega\omega} \leq 2.4\ \text{GeV} \tag{12}$$

$$B\big(\psi \to \gamma X(1.6-1.9\ \text{GeV},\ 0^-)\big) \cdot B\big(X(1.6-1.9\ \text{GeV},\ 0^-) \to \omega\omega\big)$$

$$= (6.7 \pm 1.7 \pm 2.4) \times 10^{-4} \quad .$$

The third branching fraction agrees with the corresponding branching ratio for $J/\psi \to \gamma\rho^0\rho^0$, eq. (11), as expected by SU(3) symmetry.

5. CONCLUSIONS

In summary we have studied the radiative decays $J/\psi \to \gamma K\bar{K}$ and $J/\psi \to \gamma$ vector vector ($\gamma\phi\phi$, $\gamma\rho\rho$, $\gamma\omega\omega$).

In $J/\psi \to \gamma K\bar{K}$ the $f'(1515)$, the $\theta(1700)$ and the $\xi(2200)$ are observed. The spin-parity of the f' is 2^{++} with $x = 0.7 \pm 0.1, y = 0.02 \pm 0.2$ and $\phi_x \approx \phi_y \approx 0$. The mass and width of the θ are $m_\theta = (1720 \pm 10)$ MeV and $\Gamma_\theta = (130 \pm 25)$ MeV.

The $\xi(2200)$ is observed with 4.6σ significance, $m_\xi = (2218 \pm 3 \pm 10)$ MeV, $\Gamma_\xi < 40$ MeV (95% C.L.), and $B(J/\psi \to \gamma\xi) \cdot B(\xi \to K^+K^-) = (5.8 \pm 1.8_{stat} \pm 1.5_{sys}) \times 10^{-5}$. The present statistics do not allow us to distinguish $J^{PC} = 0^{++}$, 2^{++} and 4^{++} at the 2σ level.

Upper limits for other possible decay modes of the ξ are

$$\left.\begin{array}{lcll} B(J/\psi \to \gamma\xi(2.2)) \cdot B(\xi(2.2) \to \mu^+\mu^-) & < & 7.3 \times 10^{-6} & \\ B(J/\psi \to \gamma\xi(2.2)) \cdot B(\xi(2.2) \to \pi^+\pi^-) & < & 3 \times 10^{-5} & \\ B(J/\psi \to \gamma\xi(2.2)) \cdot B(\xi(2.2) \to K^*K) & < & 2.5 \times 10^{-4} & \\ B(J/\psi \to \gamma\xi(2.2)) \cdot B(\xi(2.2) \to K^*\bar{K}^*) & < & 3 \times 10^{-4} & \\ B(J/\psi \to \gamma\xi(2.2)) \cdot B(\xi(2.2) \to \eta\eta) & < & 7 \times 10^{-5} & \\ B(J/\psi \to \gamma\xi(2.2)) \cdot B(\xi(2.2) \to p\bar{p}) & < & 6 \times 10^{-5} & \end{array}\right\} \quad 90\%\ C.L.$$

A Higgs interpretation of this resonance seems unlikely.

In $J/\psi \to \gamma\phi\phi$ the η_c is observed with $B(\eta_c \to \phi\phi) = (0.8 \pm 0.20 \pm 0.25)\%$. The η_c spin-parity has been measured for the first time as $J^P = 0^-$.

The decay $J/\psi \to \gamma 4\pi$ is observed in two modes. In a still preliminary analysis we measure $B(\psi \to \gamma\pi^+\pi^-\pi^+\pi^-) = (6 \pm 2) \times 10^{-3}$. A large $\rho\rho$ component is found around 1.5 to 1.9 GeV which has been analyzed in terms of a spin-parity analysis with different channels and has been found to be mainly due to $J^P = \text{even}^-$, most likely 0^{-+}.

The decay $J/\psi \to \gamma\omega\omega$ is observed in $J/\psi \to \gamma\pi^+\pi^-\pi^0\pi^+\pi^-\pi^0$. The $\omega\omega$ mass distribution and the shape of the χ angle distribution suggest that the structure observed around 1.6 to 1.9 GeV in $J/\psi \to \gamma\omega\omega$ is of the same origin as the one in $J/\psi \to \gamma\rho\rho$.

ACKNOWLEDGEMENTS

I would like to thank the organizers of the Moriond meeting for the pleasant atmosphere at La Plagne. I am indebted to my colleagues from the MARK III collaboration for the

support that I have received preparing this talk. In particular, I want to thank T. Burnett, K. Einsweiler, L. Köpke, J. Richman, R. Partridge, A. Spadafora, A. Seiden, W. Toki, H. J. Willutzki, and W. Wisniewski. I would like to thank M. Ogg for fruitful discussions on the Higgs interpretation of the ξ.

REFERENCES

1] Members of the MARK III Collaboration are R. M. Baltrusaitis, D. Coffman, J. Hauser, D. G. Hitlin, J. D. Richman, J. J. Russell, R. H. Schindler, *California Institute of Technology*; K. O. Bunnell, R. E. Cassell, D. H. Coward, K. F. Einsweiler, D. Hutchinson, L. Moss, R. F. Mozley, A. Odian, J. R. Roehrig, W. Toki, Y. Unno, F Villa, N. Wermes, D. E. Wisinski, *Stanford Linear Accelerator Center*; D. E. Dorfan, R. Fabrizio, F. Grancagnolo, R. P. Hamilton, C. A. Heusch, L. Köpke, J. Perrier, H. F.-W. Sadrozinski, M. Scarlatella, T. L. Schalk, A. Seiden, D. B. Smith, *University of California at Santa Cruz*; J. J. Becker, G. T. Blaylock, H. Cui, B. I. Eisenstein, G. Gladding, S. A. Plaetzer, A. L. Spadafora, J. J. Thaler, A. Wattenberg, W. J. Wisniewski, *University of Illinois at Urbana-Champaign*; J. S. Brown, T. H. Burnett, V. Cook, C. Del Papa, A. L. Duncan, P. M. Mockett, A. Nappi, J. C. Sleeman, H. J. Willutzki, *University of Washington, Seattle*.

2] For example: G. Bhanot, Phys. Lett. 101B, 95 (1981); J. F. Donoghue, K. Johnson, B. A. Li, Phys. Lett. 99B, 416 (1981); J. Coyne, P. Fishbane, S.Meshkov, Phys. Lett. 91B, 259 (1980); T. Barnes, Z. Phys. C10, 275 (1931).

3] T. Appelquist *et al.*, Phys. Rev. Lett. 34, 365 (1975); M. Chanowitz, Phys. Rev. D12, 918 (1975); L. Okun, M. Voloshin, Moscow, ITEP-95-1976 (1976).

4] M. Chanowitz, Phys. Rev. D12, 918 (1975); T. Appelquist, R. M. Barnett, K. Lane, Ann. Rev. Nucl. Sci. 28, 387 (1978).

5] K. F. Einsweiler, *Int. Europhys. Conf. on High Energy Physics, Brighton, July 20–27, 1983* and SLAC-PUB-3202; W. Toki, *11th SLAC Summer Inst. on Particle Physics, July 18–28. 1983* and SLAC-PUB-3262; D. Hitlin, *Int. Symp. on Lepton and Photon Interactions, Cornell, Aug. 4–9, 1983* and CALT-68-1071.

6] D. L. Burke *et al.*, Phys. Rev. Lett. 49, 632 (1982).

7] D. Bernstein *et al.*, SLAC-PUB-3222, submitted to Nucl. Instru. Meth. (1983).

8] J. G. Koerner, talk given at the 11th SLAC Summer Inst., July 1983, unpublished; J. G. Koerner, J. H. Kühn, H. Schneider, Phys. Lett. 120B, 444 (1982).

9] F. E. Close, Phys. Rev. D27, 311 (1983).

10] J. G. Koerner, J. H. Kühn, M. Krammer, H. Schneider, Nucl. Phys. B229, 115 (1983).

11] H. E. Haber, G. L. Kane, Phys. Lett. 135B, 196 (1984); R. S. Willey, PITT-17-83 (1983).

12] H. E. Haber, SLAC-PUB-3193, submitted to Phys. Lett. B, (1983); M. Chanowitz, Proc. X Int. Conf. on Multi-Particle Dynamics, Lake Tahoe, June 22-27, 1983; M. Chanowitz and S. Sharpe, Phys. Lett. 132B, 413 (1983); M. Shatz, Cal. Tech. Report, CALT-68-1089 (1984); K. Senba and M. Tanimoto, Ehime University Preprint, EHU-84-01 (1984); S. Godfrey, R. Kokoski, N. Isgur, Print-84-0293, Toronto (1983).

13] A. D. Linde, JETP Lett. 23, 64 (1976); Phys. Lett. 70B, 306 (1977); S. Weinberg, Phys. Rev. Lett. 36, 294 (1976).

14] F. Wilczek, Phys. Rev. Lett. 39, 1304 (1977).

15] M. Ogg, Talk presented at this conference (1984).

16] R. M. Baltrusaitis *et al.*, SLAC-PUB-3283, submitted to Phys. Rev. Lett. (1984).

17] R. Partridge *et al.*, Phys. Rev. Lett. 45, 1150 (1980).

18] N. P. Chang and C. T. Nelson, Phys. Rev. Lett. 40, 1617 (1978).

19] T. L. Trueman, Phys. Rev. D18, 3423 (1978).

20] C. N. Yang, Phys. Rev. 77, 722 (1950).

21] R. Brandelik *et al.*, Phys. Rev. Lett. 97B, 448 (1980); M. Althoff *et al.*, Z. Phys. C16, 13 (1982).

22] H. J. Behrend *et al.*, Z. Phys. C21, 205 (1984).

23] H. Kolanoski, Proc. 5th Int. Workshop on Photon Photon Interactions, Aachen, Germany, April 13-16, 1983.

24] A. Etkin *et al.*, Phys. Rev. Lett. 49, 1620 (1982); S. J. Lindenbaum, Proc. of the 1983 EPS Conference, Brighton, (1983).